Optica Applicata, Vol. XV, No. 1, 1985

Heat-spreading in light-emitting Burrus-type diodes*

Włodzimierz Nakwaski, Andrzej M. Kontkiewicz

Institute of Physics, Technical University of Łódź, ul. Wólczańska 219, 93–005 Łódź, Poland.

An analysis of a heat spreading in Burrus-type light-emitting diodes is proposed. The analysis is carried out by means of an electrical analog model. Its results are presented in numerous diagrams. They let us determine an exactness of the hitherto existing analytic thermal model of the diode and make it possible to formulate the assumptions for a new, analytical, exact, thermal model of the Burrus-type light-emitting diode. In such a model, a penetration of a heat flux into a higher-resistivity area and into a n-type layer as well as the thickness of an active layer should be taken into account.

1. Introduction

Burrus-type light emitting diode [1–3] is a fundamental source of non-coherent radiation used in fibre-optic communication systems. In order to increase the efficiency of the diode coupling with the low numerical-aperture fibre, the diameter of active region of the diode is minimized due to which the power density of the heat generated therein increases. Since the rise in temperature of the active region deteriorates the properties of diode exploitation, the appropriate heat optimization (assuring an efficient heat transfer to the diode base) of its structure is of the greatest importance.

The structure of the considered diode is shown schematically in Fig. 1. Due to the characteristic etched "well" in the n-type region, the fibre end can be brought nearer to the active region. Parameters of the standard structure of the Burrus-type diode are listed in the Table.

The aim of the present paper is to analyse heat spreading in the Burrus-type diode. The analysis will be useful in formulation of assumptions for the exact thermal model of this diode.

2. Approximate analytical model

First analytical model of heat spreading in the Burrus-type light-emitting diode has been presented by Kontkiewicz [4]. In this model, heat generated in the

* This work has been carried out under the M.R. I.5 Research Programme.

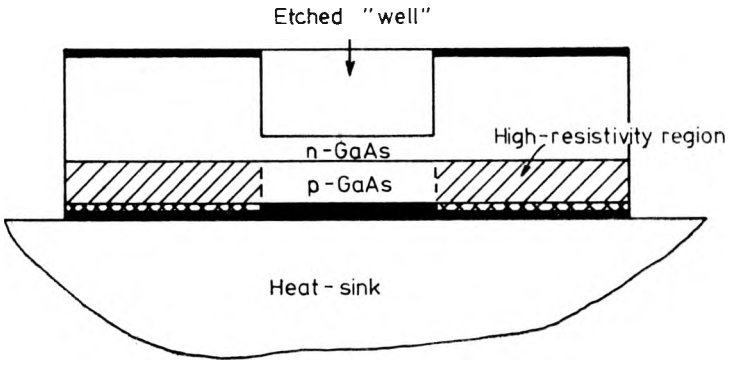

Fig. 1. Structure of Burrus-type light-emitting diode

active region (treated as a flat source) is assumed to be carried away only through p-type region. This assumption results directly from the fact that, due to high resistivity of the p-type layer neighbouring the dielectric film, the heat is generated exclusively in the junction area over the lower contact, as well as from the fact that the p-type region thickness is significantly smaller than the remaining

Parameters of the standard Burrus-type light-emitting diode

Parameter	Value	Unit
r_c	25	μm
r_s	250	μm
a	8	μm
a_0	0.25	μm
b	10	μm
c	25	μm
I	100	mA
$R_\square$	10	Ω
λ_G	47	W/mK
λ_0	1	W/mK
η_i	0.5	—

dimensions of diode and due to the presence of the mentioned dielectric film with a relatively high thermal resistance the heat spread along horizontal axis beyond the considered region is significantly limited. Hence, it can be assumed approximately that the whole heat flux, generated in the diode region enters its heat-sink directly from the p-type region.

The above assumption allows us to present the thermal equivalent circuit of the Burrus-type diode in the manner shown in Fig. 2. For this case the thermal conduction equation

$$\frac{1}{r}\frac{\partial}{r}\left(r\lambda\frac{T}{r}\right)+\frac{\partial}{\partial z}\left(\lambda\frac{\partial T}{\partial z}\right)=0 \tag{1}$$

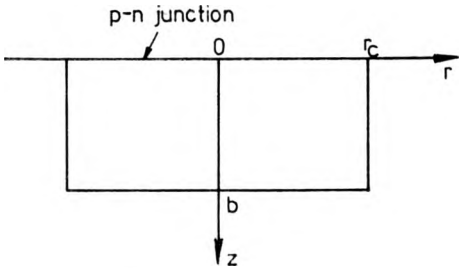

Fig. 2. Simplified thermal equivalent scheme of Burrus-type light-emitting diode

has the following boundary conditions

$$\left.\frac{\partial T}{\partial r}\right|_{r=r_c} = \left.\frac{\partial T}{\partial r}\right|_{r=0} = 0, \tag{2}$$

$$T(z = b) = T_A + \Delta T_{HS}, \tag{3}$$

$$\lambda(T)\left.\frac{\partial T}{\partial z}\right|_{z=0} = -q(r) \tag{4}$$

where r and z are cylindric coordinates (Fig. 2), T is temperature, λ – thermal conductivity, r_c – lower contact radius, b – p-type region thickness, T_A – ambient temperature, ΔT_{HS} – temperature drop on the diode heat-sink (which can be determined from the relations given in [5, 6]), $q(r)$ denotes the distribution of heat density generated in the p-n junction area.

To solve the above problem we use the Kirchhoff transformation [7]

$$\vartheta = T_A + \frac{1}{\lambda_G}\int_{T_A}^{T} \lambda(T)\,dT \tag{5}$$

where $\lambda_G = \lambda(T = T_A)$, in order to eliminate the temperature dependence of thermal conductivity. Then, the solution of Eq. (1) with the boundary conditions ((2)–(4)) obtained by separation of the variables can be written in the following form [4]:

$$\vartheta(r, z) = T_A + \Delta T_{HS} + \frac{1}{\lambda_G r_c^2}\sum_{i=1}^{\infty} B_i \sinh[K_i(b-z)]J_0(K_i r) \tag{6}$$

where K_i are the subsequent roots of the equation

$$J_1(K_i r_c) = 0, \tag{7}$$

J_0 and J_1 are the Bessel functions of the first kind of the zeroth and first orders, respectively, and the coefficients B_i are given by the relation [4]

$$B_i = \frac{1}{K_i \cosh(K_i b) J_0^2(K_i r_c)}\int_0^{r_c} q(r) r J_0(K_i r)\,dr \tag{8}$$

The heat-flux distribution $q(r)$ generated in the junction, occurring under the integral (8) and the analogous distributions of junction current density $j_{pn}(r)$ and of voltage drop $U(r)$ at the p-n junction are connected through the relation

$$q(r) = (1-\eta_i) j_{pn}(r)\, U(r) \tag{9}$$

where η_j is the internal quantum efficiency. The distributions of $j_{pn}(r)$and $U(r)$ derived by BUGAJSKI and KONTKIEWICZ [8] have the forms:

$$j_{pn}(r) = \frac{8r_c^2}{\beta R_\square} \frac{1+\xi}{[r_c^2(1+\xi)-r^2]^2}, \tag{10}$$

$$U(r) = U_A + \frac{2}{\beta} \ln \left| \frac{r_c^2 \xi}{r_c^2(1+\xi)-r^2} \right| \tag{11}$$

where

$$U_A = \frac{1}{\beta} \ln \left[\frac{I}{j_s \pi r_c^2} \left(1 + \frac{1}{\xi}\right)\right], \tag{12}$$

$$\xi = \frac{8\pi}{\beta R_\square I}, \tag{13}$$

$$\beta = \frac{e}{n_c k_B T}. \tag{14}$$

In the above relations, I denotes the total current flowing through the diode, j_s is the saturation current density, $R_\square$ – the resistance per square of the n-type layer over the p-n junction, e – electron charge, k_B – Boltzmann constant, and n_c is a constant which for GaAs electroluminescent diodes is approximately equal to 2 [9].

The model considered in the present Section may be generalized for the case in which heat flow through the n-type region is taken into account [10].

3. Analog electrical model

The main shortcoming of the thermal analytical model of the Burrus-type light-emitting diode presented above is that the heat-flux penetration into a high-resistivity p-type layer has been neglected. This penetration is limited significantly by a relatively high thermal resistance of the dielectric film, the thermal conductivity of which is almost 50 times smaller than that of semiconductor (cf. Tab.). Nevertheless, it should be remembered that because of the cylindric geometry of the device the thermal resistance decreases in reverse-proportion to the increasing distance r from the device axis. Similarly, the thermal resistivity of the high-resistance layer decreases as well. As a result, the heat-flux penetration into regions not directly adjoining metallic contact essentially influences the temperature distribution in the active region.

The heat-flux spreading in the diode will be studied by means of the analog electrical model. To this end we divide the diode structure into M prisms the shape of which is shown in Fig. 3; and choose the angle $\Delta\varphi$ sufficiently small to

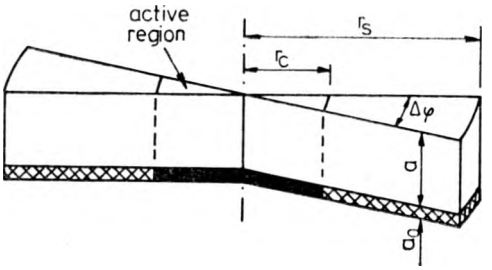

Fig. 3. Shape of one of M prisms into which the Burrus-type diode structure has been derived in the analog electrical model

treat the arc $r\Delta\varphi$ as a segment of a straight line for all r's. Due to the structure symmetry, the heat generated inside the considered prism is assumed to escape only through its heat-sink. We cannot, however, neglect the mutual heat transmission through the prism narrowing, since, e.g., in the case of a uniform heat source ($q = \text{const}$, for $r < r_c$) the calculated heat flux of the maximal density would penetrate into the heat-sink at the point $r \neq 0$.

The prism is divided into $2N+1$ segments (Fig. 4)

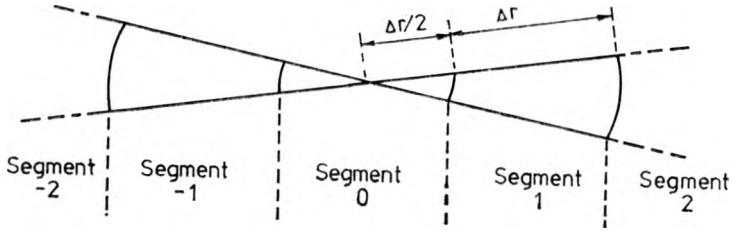

Fig. 4. Division of the prism into segments in the analog electrical model of heat spreading in Burrus-type diode

$$\Delta r = \frac{2r_s}{2N+1} \tag{15}$$

hence the radius of the lower contact

$$r_c = (n+1/2)\,\Delta r. \tag{16}$$

Then, the analog electrical model of heat spreading in the prism is shown in Fig. 5, where the respective resistivities may be expressed by the following relations:

$$R_1^k = \frac{2}{b\lambda_G \Delta\varphi(2|k|-1)}, \quad k \in \langle -N, -1\rangle \text{ or } k \in \langle 1, N\rangle \tag{17}$$

$$R_2^k = \frac{b}{\lambda_G \Delta\varphi(\Delta r)^2 |k|}, \quad k \in \langle -N, -1\rangle \text{ or } k \in \langle 1, N\rangle \tag{18}$$

$$R_2^0 = \frac{2b}{\lambda_G \Delta\varphi(\Delta r)^2}, \tag{19}$$

$$R_0^k = \frac{a_0}{\lambda_0 \Delta\varphi(\Delta r)^2 |k|}, \quad k \in \langle -N, -n-1\rangle \text{ or } k \in \langle n+1, N\rangle. \tag{20}$$

In the above relations, a_0 and λ_0 are, respectively, dielectric-film thickness and its thermal conductivity.

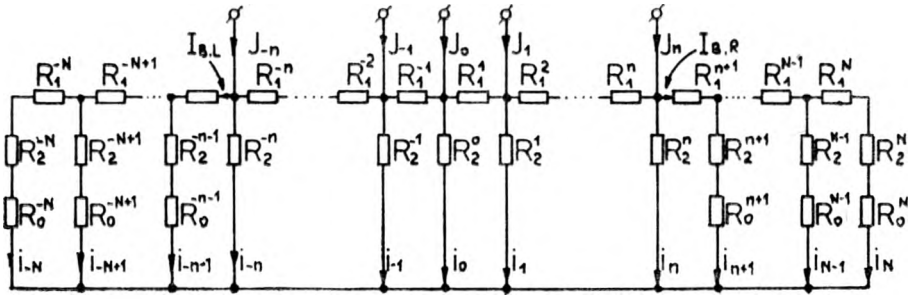

Fig. 5. Analog electrical model of heat spreading in Burrus-type diode

Then, the current-density distribution, being the analog equivalent of the density of heat flux generated in the active region, will be the following:

$$J_k = q(r = |k|\,\Delta r). \tag{21}$$

To conduct further calculations it is necessary to determine the equivalent resistence (R_{ch}) of four-terminal network chain beyond the active region:

$$R_N = R_2^N + R_0^N, \tag{22}$$

$$R_k = \frac{(R_2^k + R_0^k)(R_1^{k+1} + R_{k+1})}{R_1^{k+1} + R_2^k + R_0^k + R_{k+1}}, \quad k \in \langle n+1, N\rangle \tag{23}$$

$$R_{ch} = R_{n+1} = R_{-n-1}. \tag{24}$$

Further calculations are based on the current-source superposition rule (Fig. 6):

$$R_{ch,-n}^L = R_1^{-n-1} + R_{ch}, \tag{25}$$

$$R_{ch,k}^L = R_1^{k-1} + \frac{R_2^{k-1} R_{ch,k-1}^L}{R_2^{k-1} + R_{ch,k-1}^L}, \quad k \in \langle -n+1, 0\rangle \tag{26}$$

$$R_{ch,k}^L = R_1^k + \frac{R_2^{k-1} R_{ch,k-1}^L}{R_2^{k-1} + R_{ch,k-1}^L}, \quad k \in \langle 1, n\rangle \tag{27}$$

$$R^{\mathrm{R}}_{\mathrm{ch},n} = R_1^{n+1} + R_{\mathrm{ch}}, \tag{28}$$

$$R^{\mathrm{R}}_{\mathrm{ch},k} = R_1^{k+1} + \frac{R_2^{k+1} R^{\mathrm{R}}_{\mathrm{ch},k+1}}{R_2^{k+1} + R^{\mathrm{R}}_{\mathrm{ch},k+1}}, \qquad k \in \langle 0, n-1 \rangle \tag{29}$$

$$R^{\mathrm{R}}_{\mathrm{ch},k} = R_1^{k} + \frac{R_2^{k+1} R^{\mathrm{R}}_{\mathrm{ch},k+1}}{R_2^{k+1} + R^{\mathrm{R}}_{\mathrm{ch},k+1}}, \qquad k \in \langle -n, 1 \rangle \tag{30}$$

$$i_{k,k} = J_k \frac{R_{z,k}}{R_2^k + R_{z,k}}, \qquad k \in \langle -n, n \rangle \tag{31}$$

$$R_{z,k} = \frac{R^{\mathrm{L}}_{\mathrm{ch},k} R^{\mathrm{R}}_{\mathrm{ch},k}}{R^{\mathrm{L}}_{\mathrm{ch},k} + R^{\mathrm{R}}_{\mathrm{ch},k}}, \qquad k \in \langle -n, n \rangle \tag{32}$$

$$i_{\mathrm{L},k} = (J_k - i_{k,k}) \frac{R^{\mathrm{R}}_{\mathrm{ch},k}}{R^{\mathrm{L}}_{\mathrm{ch},k} + R^{\mathrm{R}}_{\mathrm{ch},k}}, \qquad k \in \langle -n, n \rangle \tag{33}$$

$$i_{\mathrm{R},k} = J_k - i_{k,k} - i_{\mathrm{L},k}, \qquad k \in \langle -n, n \rangle \tag{34}$$

$$I_{\mathrm{R},k} = i_{\mathrm{R},k} - \sum_{\nu=1}^{n-k} i_{k+\nu,k}, \qquad k \in \langle -n, n \rangle \tag{35}$$

$$I_{\mathrm{L},k} = i_{\mathrm{L},k} - \sum_{\nu=1}^{n+k} i_{k-\nu,k}, \qquad k \in \langle -n, n \rangle \tag{36}$$

Whence, the heat-flux spreading under the active region can be determined

$$i_{k+\nu,k} = \left(i_{\mathrm{R},k} - \sum_{\nu=1}^{\nu-1} i_{k+\nu',k} \right) \frac{R^{\mathrm{R}}_{\mathrm{ch},k+\nu}}{R_2^{k+\nu} + R^{\mathrm{R}}_{\mathrm{ch},k+\nu}}, \qquad \nu \in \langle 1, n-k \rangle \tag{37}$$

$$i_{k-\nu,k} = \left(i_{\mathrm{L},k} - \sum_{\nu=1}^{\nu-1} i_{k-\nu,k} \right) \frac{R^{\mathrm{L}}_{\mathrm{ch},k-\nu}}{R_2^{k-\nu} + R^{\mathrm{L}}_{\mathrm{ch},k-\nu'}}, \qquad \nu \in \langle 1, k+n \rangle \tag{38}$$

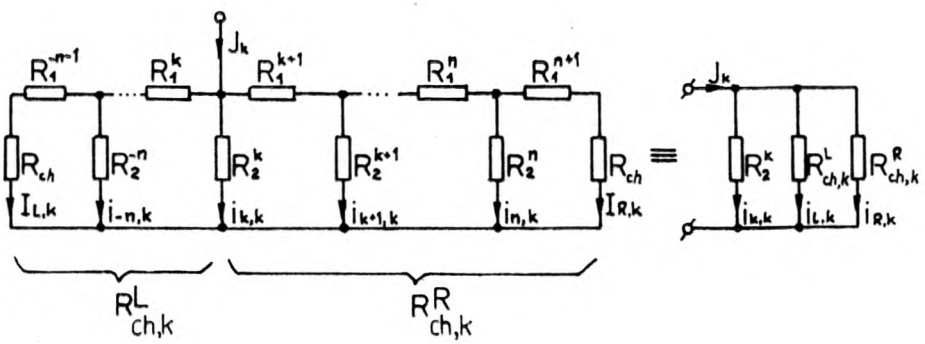

Fig. 6. Application of the superposition rule of current sources (for $k > 0$) in the analog electrical model of heat spreading in Burrus-type diode

$$I_{\mathrm{B,R}} = \sum_{k=-n}^{n} I_{\mathrm{R},k}, \tag{39}$$

$$I_{\mathrm{B,L}} = \sum_{k=-n}^{n} I_{\mathrm{L},k} = I_{\mathrm{B,R}}, \tag{40}$$

$$i_k = \sum_{k'=-n}^{n} i_{k,k'}, \qquad k \in \langle -n, n \rangle \tag{41}$$

and next this spreading beyond the active region:

$$i_k = \left(I_{\mathrm{B,R}} - \sum_{k'=n+1}^{k-1} i_{k'}\right) \frac{R_1^{k+1} + R_{k+1}}{R_1^{k+1} + R_2^k + R_0^k + R_{k+1}}, \qquad k \in \langle n+1, N-1 \rangle \tag{42}$$

$$i_{\mathrm{N}} = I_{\mathrm{B,R}} - \sum_{k'=n+1}^{N-1} i_{k'}. \tag{43}$$

4. Results

Results of the above calculations for a standard Burrus-type electroluminescent diode with parameters listed in the Table are illustrated in the subsequent figures. For instance, the distribution of current density $j_{\mathrm{pn}}(r)$ flowing through the p-n junction, that of voltage drop $U(r)$ on the junction, as well as of the density $q(r)$ of heat flux generated in the junction plane and represented by J_k in the analog model (cf. (21)) are shown in Fig. 7.

The changes in R_1, R_2 and R_0, forming the considered analog electrical model of the heat-flux spreading in Burrus-type diode, are presented in logarithmic scale in Fig. 8. Attention should be paid to the rapidly decreasing resistance with the increasing distance from the diode axis.

Distribution of density of the heat flux $q_{\mathrm{HS}}(r)$ in the Burrus-type diode penetrating into heat-sink is given in Fig. 9. In the analog model this flow is represented by current density

$$J_{\mathrm{HS},k} = i_k \frac{\lambda_{\mathrm{G}} R_2^k}{b}. \tag{44}$$

For comparison, the distribution $q(r)$ has been also shown with the broken line. The plot given in this figure confirms our hypothesis that heat-flux penetration into the high-resistance region plays essential part in the whole process of heat spreading occurring in the Burrus-diode. Comparison of the distributions $q(r)$, $q_{\mathrm{HS}}(r)$ in the region directly over the lower contact ($r < r_{\mathrm{c}}$) is also of interest. It appears that the heat-flux spreading in the Burrus-type diode partially decreases nonuniformity of heat-flux distribution in the active region. Hence, $q_{\mathrm{HS}}\ (r = 0) > q(r = 0)$, whereas $q_{\mathrm{HS}}(r = r_{\mathrm{c}}) < q(r = r_{\mathrm{c}})$.

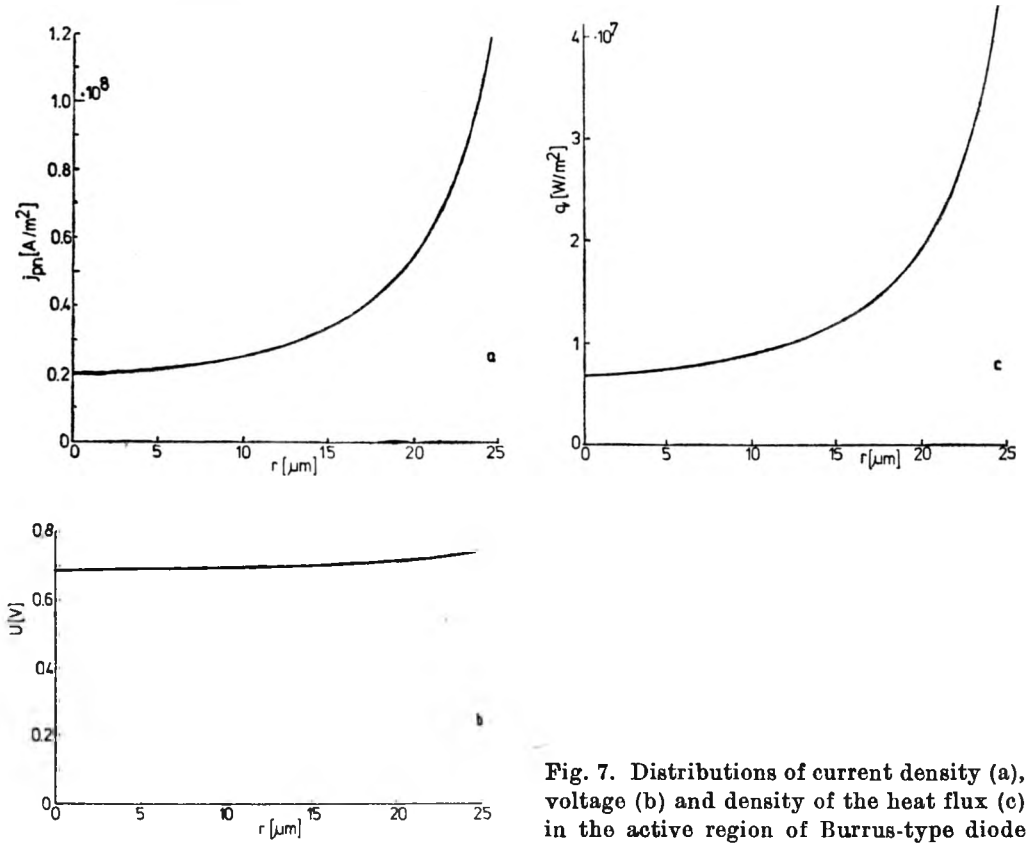

Fig. 7. Distributions of current density (a), voltage (b) and density of the heat flux (c) in the active region of Burrus-type diode

The most important result of the analysis of heat spreading in the Burrus-type diode area based on the above analog model of this spreading (Sec. 3) is that the heat flux penetrating into the high-resistivity region has been determined.

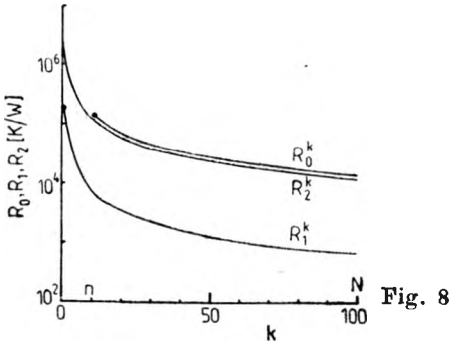

Fig. 8

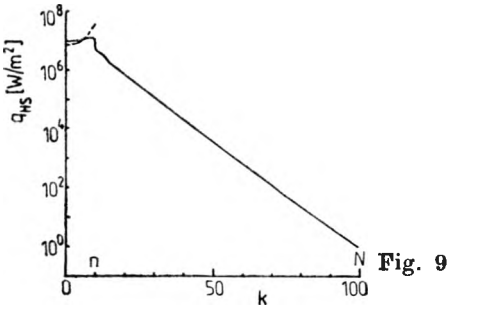

Fig. 9

Fig. 8. Distributions of the resistance values R_0, R_1, R_2 in the analog electrical model of the standard Burrus-type diode ($\Delta\varphi = \pi/100$)

Fig. 9. Distributions of a density of heat flux $q_{HS}(r)$ penetrating from the standard Burrus-type diode area into the heat-sink. Dashed line denotes the distribution $q(r)$ of density of heat flux generated in the active region

The distribution of density of the heat flux $q'(r)$ generated in the diode active region and not penetrating into the high-resistivity region, and being remained in the region considered in the previous model (Sec. 2) is given in Fig. 10. In the analog model this flow is represented by current density

$$J'_k = J_k - (I_{R,k} + I_{L,k}) \frac{\lambda_G R_2^k}{c}. \tag{45}$$

Figure 10 confirms the hypothesis that neglecting heat-flux penetration into the high-resistivity region gives use to a significant error. For instance, more than one half (ca 53%) of the heat flux, generated in the most efficient heat-flux emission region situated near the active region edge, penetrates into the high-resistivity region; thus in practice, it does not take part in the heat-flux spreading directly under the active region, considered in the former model.

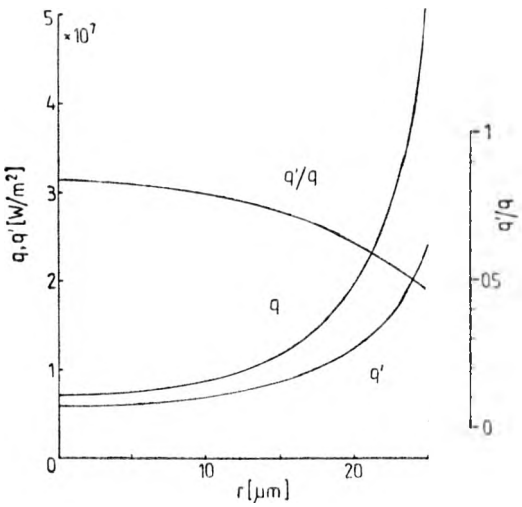

Fig. 10. Distributions of a density of heat flux $q(r)$ generated in the active region of the standard Burrus-type diode and of heat flux $q'(r)$ being a part of the flux $q(r)$ which does not penetrate into the high-resistivity region ($r > r_c$)

The subsequent plots illustrate the influence of the structural parameters of the Burrus-type diode on the heat-flux spreading in its area. For instance, Fig. 11 shows the influence of the dielectric-film thickness a_0 on the distribution of heat-flux q', not penetrating into the high-resistivity region ($r > r_c$). It appears that this influence is considerably smaller than the expected one. When the thickness was reduced ten times (from 0.5 μm to 0.05 μm) the value of q'/q ratio only slightly decreased (from 0.51 to 0.41), for $r = r_c$. Even a total removal of that film ($a_0 = 0$) does not improve radically thermal properties of the Burrus-type diode, since then above ratio equals 0.38.

The spreading of heat flux generated in the diode active region depends to a much higher degree on the thickness b of the p-type layer between the active region and the lower contact. This effect is illustrated in Fig. 12. It can be seen that for small thickness of this layer ($b = 2$ μm or 5 μm) the distribution of heat flux density, $q'(r)$, inside the active region only slightly differs from $q(r)$. With the increasing value of b the heat-flux spread is distinctly facilitated, the dif-

ference between $q'(r)$, and $q(r)$ substantially increases and the nonuniformity of the former distribution decreases. With the increasing values of b the values of R_1 decrease (Eq. (17)) and those of R_2 increase (Eq. (18)). Hence, it follows that the effect of the R_1 resistance on the run of the analysed process is higher.

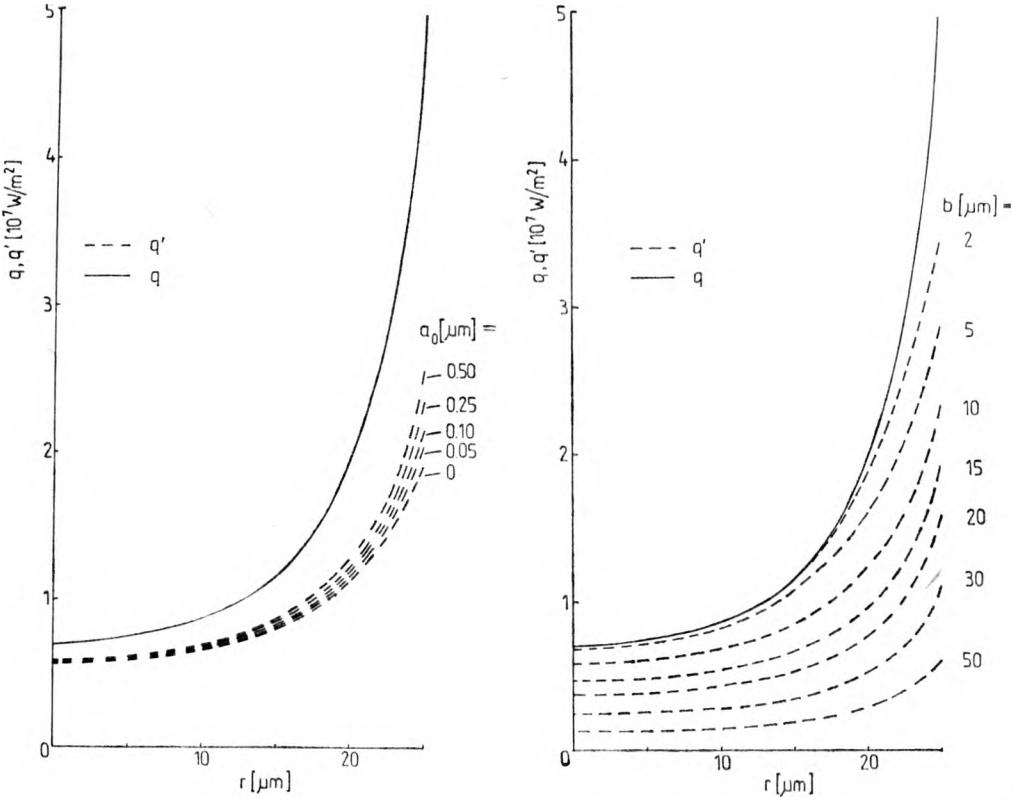

Fig. 11. Influence of the thickness a_0 of the dielectric film on the heat-flux distribution q' in the standard Burrus-type diode

Fig. 12. Influence of the thickness b of the p-type layer between the active region and the lower contact on the heat-flux distribution q' in the standard Burrus-type diode

The influence of another structural parameter of the diode, namely of the resistance per square $R_\square$, of the n-type layer between the upper contact and the active region, is shown in Fig. 13. In this figure the distributions of densities of the heat flux $q(r)$, generated in the active region are given for $R_\square$ ranging from 1Ω to 50Ω. According to our expectations the parameter substantially influences the $q(r)$ distribution. Its nonuniformity expressed by the $q(r = r_c)$ to $q(r = 0)$ ratio is for $R_\square = 1\Omega$ equal to 1.34, whereas for $R_\square = 50\Omega$ $q/q' = 98$. For all the values of $R_\square$ distribution of this ratio is identical. Hence, the $q'(r = r_c)/q'(r = 0)$ ratio, i.e., the measure of nonuniformity of the q' distribution, is for $R = 1\Omega$ even less than one, i.e., equal to 0.73, reaching the value of 55, when $R_\square = 50\Omega$.

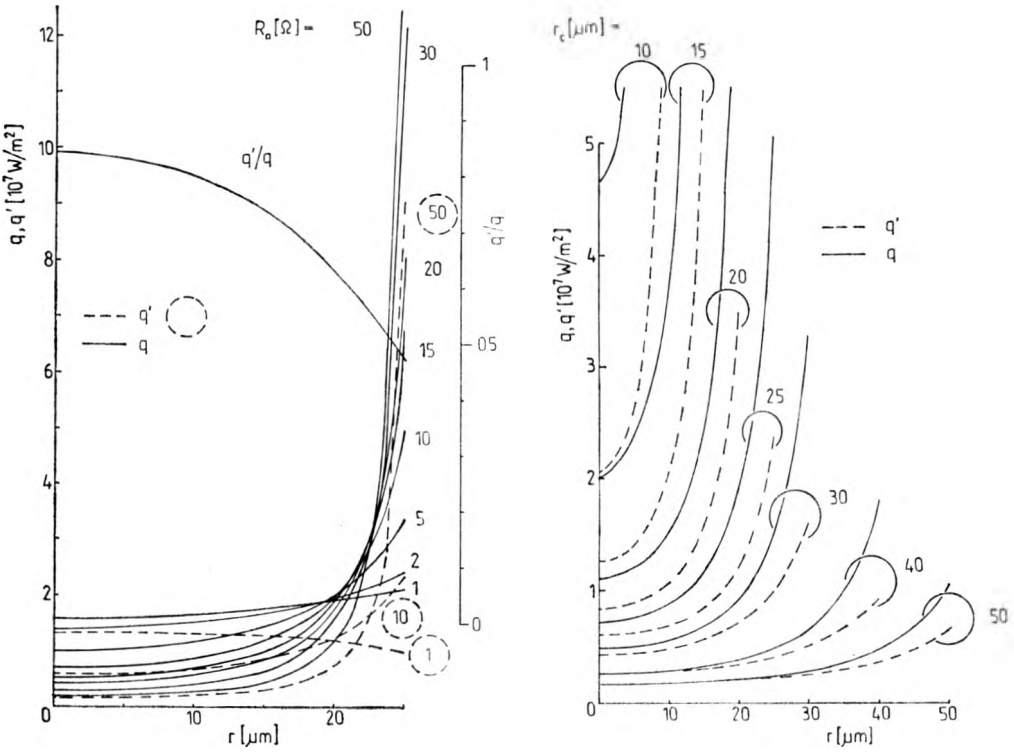

Fig. 13. Influence of the resistance per square $R_{\square}$ of the n-type layer on the distributions of heat flux densities q and q' in the standard Burrus-type diode

Fig. 14. Influence of the radius r_c of the lower contact on the distributions of heat flux densities q and q' in the standard Burrus-type diode

Another structural parameter, influencing to a considerable extent the distribution $q(r)$ and $q'(r)$, is the radius r_c of the lower contact. This effect is obvious because of the assumed constant supply current $I = 100$ mA (see Table). This influence is shown in Fig. 14, whereas the influence of the above radius on the distribution of q'/q ratio is given in Fig. 15. The obtained curves are approximately parallel, i.e., they are shifted along the r-coordinate and slightly raised along the z-coordinate. If the heat-flux flow in the direction opposite to r-axis had been omitted in the calculations, these curves would have been ideally parallel, i.e., they would have been shifted along the r-coordinate only. Hence, it follows that the increasing of the q'/q ratio (for $r = r_c$) with increasing r_c illustrates the increased relative contribution of the above flow in the total heat-spreading process in the Burrus-type diode.

The influence of increasing supply current (I) on the distributions $q'(r)$ is presented in Fig. 16. It can be seen that, for low supply currents the distribution $q'(r)$ is almost uniform within the whole active region. With the increasing values of current I, $q'(r = r_c)$ increases rapidly, the q' distribution near the diode axis being practically unchanged. This fact should be taken into account

in design of a power-supply unit for the Burrus-type diode. Each increase in the supply current influences the increase in heat-source rate in neighbourhood of the active-region edge, only, thus, increasing the nonuniformity of the distri-

Fig. 15 ▼

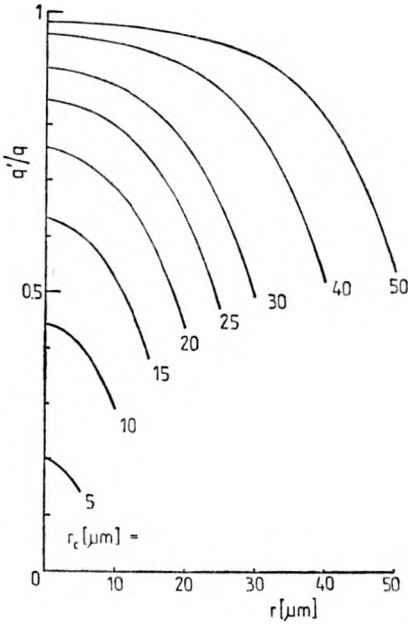

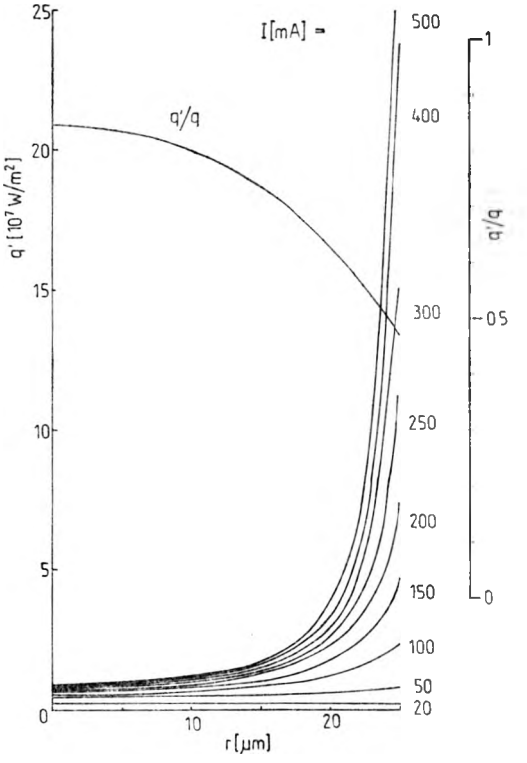

Fig. 15. Dependence of distribution of q'/q ratio upon the radius r_c of the lower contact in the standard Burrus-type diode

Fig. 16. Influence of supply-current value I on the distribution of heat flux density q' in the standard Burrus-type diode

bution. This, in turn, results in the increasing temperature-distribution nonuniformities that through the anti-guiding effect deteriorates the diode-fibre coupling efficiency. The increase in the nonuniformities of $q(r)$ and $q'(r)$ distributions due to the supply-current increase are clearly seen in Fig. 17.

5. Discussion

The results of the analog model of the heat spreading in the Burrus-type diode allow us to estimate the accuracy of the approximations applied in the former analytical model, and make it possible to formulate the assumptions for a more accurate model. The conclusions resulting from the above analysis may be expressed as follows:

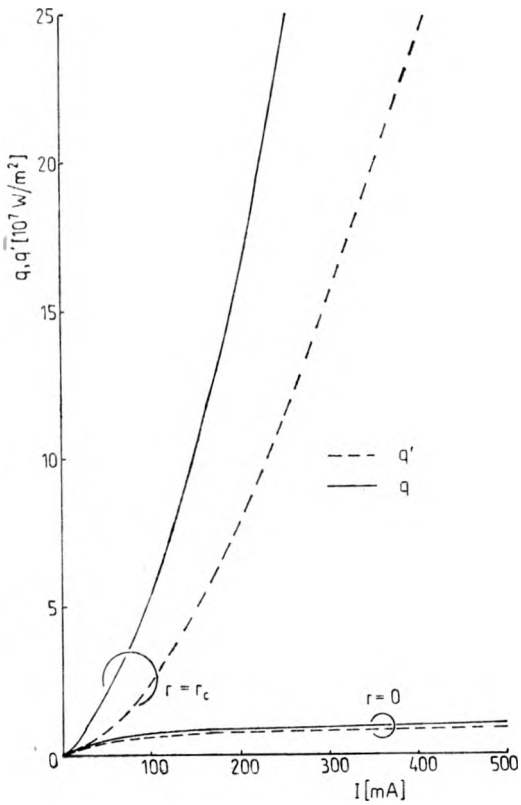

Fig. 17. Dependence of densities of heat flux q and q' in the centre and at the edge of the active region upon the value of supply current in the standard Burrus-type diode

1. The omission of heat-flux penetration into the high-resistivity region (Fig. 18), i.e., assumption of the boundary condition in the form

$$\left.\frac{\partial T}{\partial r}\right|_{r=r_0} = 0, \tag{46}$$

leads to a significant error. The temperature distributions calculated under this assumption are distinctly overestimated, in particular, in neighbourhood of the active-region edge.

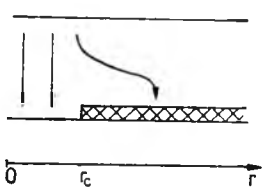

Fig. 18

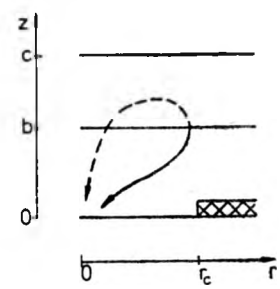

Fig. 19

Fig. 18. Penetration of heat flux into the high-resistivity region of the Burrus-type diode

Fig. 19. Heat flow from its efficient generation region in neighbourhood of the active-region edge to the Burrus-type diode centre

A relative contribution of this penetration into the whole heat-spreading process occurring in the Burrus-type diode depends, of course, upon its structure. It should be noticed, however, that in the case of a standard structure of the diode (see Table) about 53% of the heat flux generated in the neighbourhood of the active-region edge (i.e., the region characterized by the most efficient heat generation) penetrates into the high-resistivity region. This percentage decreases when moving deeper into the active region, but even in its centre it equals about 16%. The importance of the above effect increases substantially with the increasing supply current, resistance per square of the n-type layer, and/or the thickness of the p-type layer, as well as with the decreasing radius of the lower contact, whereas the impact of a reasonably increased thickness of dielectric film is much smaller. This is due to the fact that thermal resistances of the high-resistivity region and dielectric film (their equivalents in the analog model being the resistances R_1, R_2 and R_0) decrease rapidly with the increasing distance from the active region, thus, due to a cylindrical symmetry of the diode structure which promotes the heat-flux spreading in horizontal direction (along the r-axis).

The situation is quite different in the case of oxide-insulated stripe lasers [11] characterized by Cartesian symmetry, in which the heat-flux spreading in the lateral direction is greatly limited [12]. The shape of the heat flux density in the active region is an additional factor diminishing this spreading, since (opposite to the case of the Burrus-type diode) the most efficient heat generation occurs in the centre of the active region. Moreover, a much smaller distance between the active region and the heat-sink, when compared with the Burrus-type diode dimensions (Fig. 12), also limits the considered heat-flux spreading.

2. From the comparison of distributions of the heat-flux $q_{HS}(r)$ penetrating into the Burrus-type diode heat-sink and of the heat flux $q(r)$ generated in the diode active region (Fig. 9), as well as from the comparison of heat-flux ratio $q'/q(r = r_c)$ for various radii of the lower contact (Fig. 15), it follows that the flow of heat flux from the efficient heat-generation region (near to the active-region edge) towards the diode centre contributes substantially to the whole heat-flux spreading. This flow is particularly significant in the case of high nonuniformity of distribution of a density of heat flux generated in the active region, taking place just in the Burrus-type diode. In the hitherto analytical model the above effect has been artificially limited by neglecting the penetration of heat-flux into the n-type region (broken line in Fig. 19). In the generalized version of this model [10] this penetration will be taken into account.

3. A substantial influence of the distance of the generation point from the diode heat-sink on the heat-spreading process in the device is shown in Fig. 12. This conclusion contradicts the assumption of the planar heat source taken in the previous model. Thus the model accuracy may be improved by taking account of the real thickness ($b - a \approx 2$ μm, Fig. 20) of the active region.

The above results will be used in formulation of a more accurate analytical thermal model of the Burrus-type diode, which will be the subject of a separate

paper. It should be, however, emphasized that the future model will be more complicated, thus, requiring the application of numerical methods. The model presented in Sec. 2 can be still used for fast approximate calculations, bearing in mind that this model does not take account of heat-flux penetration into the

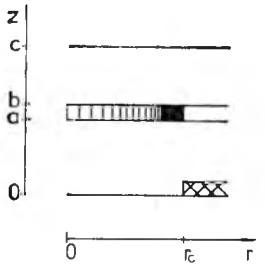

Fig. 20. Taking account of the active-region thickness in the thermal model of the Burrus-type diode

high-resistivity region and the n-type layer, and it neglects a space-spread of the heat source in the active region, and for these reasons the temperature distributions (especially, in the neighbourhood of the active region) are overestimated.

6. Conclusions

The analysis of a heat-flux spreading in the Burrus-type diode, presented in this paper and performed by using an analog electrical model, enables the formulation of the following conclusions:

i) An accurate thermal model of the Burrus-type diode should take account of the heat-flux penetration into the high-resistivity region, despite an additionally occurring thermal resistance of the dielectric film.

ii) The heat sources in this model should be placed deep in the considered diode region, and not at its edge.

iii) The model accuracy can be improved if the active-region thickness is taken into account.

Acknowledgements – The authors would like to thank Professor Bohdan Mroziewicz from the Institute of Electron Technology, Warsaw, for many fruitful discussions.

References

[1] BURRUS C. A., MILLER B. I., Opt. Commun. **4** (1971), 307.
[2] BURRUS C. A., Proc. IEEE **60** (1972), 231.
[3] DAREK B., LIPIŃSKI T., KONTKIEWICZ A. M., Prace ITE, No. 1 (1979), 89 (in Polish).
[4] KONTKIEWICZ A. M., Prace ITE, No. 5 (1983), 15 (in Polish).
[5] NAKWASKI W., Solid-St. Electron., in press.
[6] NAKWASKI W., Optica Applicata, in press.
[7] KIRCHHOFF G. R., *Vorlesungen über die Theorie der Wärme*, 1894, and CARSLAW H. S., JAEGER J. C., *Conduction of Heat in Solids*, Clarendon Press, Oxford 1959, p. 11.
[8] BUGAJSKI M., KONTKIEWICZ A. M., Electron Technology **13** (1982), No. 4, p. 63.

[9] DUMIN D. J., PEARSON G. L., J. Appl. Phys. **36** (1965), 3418.
[10] KONTKIEWICZ A. M., in preparation.
[11] NAKWASKI W., Rozprawy Elektrotechniczne **29** (1983), 611 (in Polish).
[12] NAKWASKI W., Opt. Quant. Electron, in press.

Received July 27, 1984

Теплообмен в полупроводниковом светоизлучающем диоде Барраса

В настоящей работе представлен анализ теплообмена в полупроводниковом светоизлучающем диоде Барраса. Этот анализ произведен с помощью аналоговой электрической модели. Результаты модели представлены на многочисленных диаграммах. Они делают возможными определение точности существовавшей до сих пор аналитической тепловой модели полупроводникового светоизлучающего диода Барраса, а также формулировку предположения для новой, аналитической, точной, тепловой модели этого диода. В этой модели должна быть учтена толщина активной области, а также вникание потока тепла в побочный слой высокого сопротивления и в слой *n*-типа.